Lecture Notes: Three-Level Systems and Defect Centers

Dark states, shelving, NV centers, ODMR, and magnetometry

Contents

1 Bridge: from two-level systems (TLS) to three-level systems (3LS)

1.1 Minimal TLS recap (so we can reuse the machinery)

A TLS has basis $\{|g\rangle, |e\rangle\}$ with bare Hamiltonian

$$\hat{H}_0 = E_g |g\rangle\langle g| + E_e |e\rangle\langle e|, \qquad \hbar\omega_0 = E_e - E_g. \tag{1}$$

Driven (semi-classical) by a monochromatic field $E(t) = E_0 \cos(\omega t)$, the dipole interaction is

$$\hat{V}(t) = -\hat{\boldsymbol{\mu}} \cdot \boldsymbol{E}(t). \tag{2}$$

With dipole matrix element $\mu_{ge} = \langle g|\hat{\boldsymbol{\mu}} \cdot \hat{\boldsymbol{e}}|e\rangle$, one defines the (on-resonance) Rabi frequency

$$\Omega \equiv \frac{\mu_{ge} E_0}{\hbar}. \tag{3}$$

Under RWA and in the rotating frame, a standard TLS Hamiltonian is

$$\hat{H}_{\mathrm{TLS}}^{(\mathrm{rot})} = \frac{\hbar}{2}(\Delta\,\sigma_z + \Omega\,\sigma_x), \qquad \Delta \equiv \omega - \omega_0. \tag{4}$$

Logic note (for lecture): Why revisit TLS?

Every multi-level derivation will reuse the same steps: (i) choose a basis, (ii) write $\hat{H}_0$, (iii) write $\hat{V}(t)$ from dipole coupling, (iv) go to a rotating frame, (v) apply RWA $\Rightarrow$ slowly-varying coupled equations.

1.2 Why introduce a third level? (new physics)

A third level can introduce:

- **Coherent interference** between two excitation pathways (true *dark states* in Λ systems).
- **Incoherent shelving** into a metastable state ("dark" fluorescence state).
- **Optical pumping** and **spin polarization** mechanisms (especially in defect centers).

Key point: Two kinds of "dark states"

Coherent dark state (CPT/EIT): a superposition decoupled from light by destructive interference.
Incoherent dark (shelved) state: population trapped in a long-lived state that does not fluoresce.

2 Three-level systems (3LS): Λ, V, and Ξ topologies

2.1 Three canonical configurations

We label three bare energy eigenstates $\{|1\rangle, |2\rangle, |3\rangle\}$ with energies $E_1 < E_2 < E_3$.

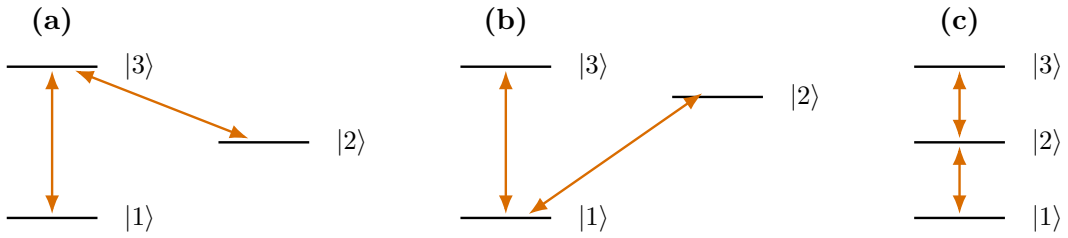

Figure 1: Correct three-level topologies: (a) Λ-type, (b) V-type, (c) cascade (Ξ)-type. Arrows indicate allowed transitions.

Info: Topologies

Λ system: two lower states $|1\rangle, |2\rangle$ coupled to a common excited $|3\rangle$.
V system: one ground $|1\rangle$ coupled to two excited states $|2\rangle, |3\rangle$.
Cascade (Ξ) system: ladder $|1\rangle \leftrightarrow |2\rangle \leftrightarrow |3\rangle$.

In what follows we will focus heavily on the Λ system because it naturally supports *coherent dark states*. Later, we connect to NV centers where "dark" behavior commonly appears via *shelving* (incoherent dark state).

2.2 General 3LS Hamiltonian and dipole interaction

Bare Hamiltonian:

$$\hat{H}_0 = \sum_{j=1}^{3} E_j \, |j\rangle\langle j| \, . \tag{5}$$

Assume the atom (or emitter) is driven by (up to) two classical fields:

$$\boldsymbol{E}_1(t) = \hat{\boldsymbol{e}}_1 E_1 \cos(\omega_1 t + \phi_1), \tag{6}$$
$$\boldsymbol{E}_2(t) = \hat{\boldsymbol{e}}_2 E_2 \cos(\omega_2 t + \phi_2). \tag{7}$$

Dipole coupling (electric dipole approximation):

$$\hat{V}(t) = -\hat{\boldsymbol{\mu}} \cdot (\boldsymbol{E}_1(t) + \boldsymbol{E}_2(t)). \tag{8}$$

Define dipole matrix elements

$$\mu_{ij}^{(k)} \equiv \langle i|\hat{\boldsymbol{\mu}} \cdot \hat{\boldsymbol{e}}_k|j\rangle \, , \quad k \in \{1, 2\}. \tag{9}$$

Logic note (for lecture): What to emphasize

The 3LS structure is not just "more levels"; it changes interference and opens additional decay routes.

3 Λ system in detail: coherent dark states and CPT

3.1 Setup and RWA Hamiltonian

Consider a Λ system with allowed optical transitions

$$|1\rangle \leftrightarrow |3\rangle \, , \qquad |2\rangle \leftrightarrow |3\rangle \, ,$$

and forbidden (or very weak) direct $|1\rangle \leftrightarrow |2\rangle$ optical transition.

We drive:

- field 1 at frequency ω_1 couples $|1\rangle \leftrightarrow |3\rangle$,
- field 2 at frequency ω_2 couples $|2\rangle \leftrightarrow |3\rangle$.

Define transition frequencies:

$$\omega_{31} \equiv \frac{E_3 - E_1}{\hbar}, \qquad \omega_{32} \equiv \frac{E_3 - E_2}{\hbar}. \tag{10}$$

Define detunings:

$$\Delta_1 \equiv \omega_1 - \omega_{31}, \qquad \Delta_2 \equiv \omega_2 - \omega_{32}. \tag{11}$$

Define **two-photon detuning**:

$$\delta \equiv \Delta_1 - \Delta_2 = (\omega_1 - \omega_2) - (\omega_{31} - \omega_{32}) = (\omega_1 - \omega_2) - \frac{E_2 - E_1}{\hbar}. \tag{12}$$

Define (complex) Rabi frequencies (including phases):

$$\Omega_1 \equiv \frac{\mu_{31}^{(1)} E_1}{\hbar} e^{i\phi_1}, \qquad \Omega_2 \equiv \frac{\mu_{32}^{(2)} E_2}{\hbar} e^{i\phi_2}. \tag{13}$$

Under a standard rotating-frame transformation and RWA, the interaction Hamiltonian can be written (one common convention) as

$$\hat{H}_\Lambda^{(\mathrm{rot})} = -\hbar\Delta_1 |3\rangle\langle 3| - \hbar\delta |2\rangle\langle 2| + \frac{\hbar}{2} \left(\Omega_1 |3\rangle\langle 1| + \Omega_2 |3\rangle\langle 2| + \mathrm{h.c.}\right). \tag{14}$$

Info: Convention note

Different books choose different zero-energy references. The physics is invariant. What matters: detunings appear on diagonal terms; couplings appear off-diagonal with $\Omega_{1,2}$.

3.2 Derive the dark state (all algebra steps)

A **dark state** is an eigenstate of the driven system that has *no component on the radiative excited state* $|3\rangle$, so it does not absorb light and does not fluoresce.

Let a general state in the lower manifold be

$$|\psi\rangle = a\,|1\rangle + b\,|2\rangle\,. \tag{15}$$

We ask: when is $|\psi\rangle$ uncoupled from $|3\rangle$ by the interaction part of (14)?

The coupling from $|1\rangle, |2\rangle$ to $|3\rangle$ is:

$$\hat{H}_{\mathrm{cpl}} = \frac{\hbar}{2} \left(\Omega_1 |3\rangle\langle 1| + \Omega_2 |3\rangle\langle 2| + \mathrm{h.c.}\right). \tag{16}$$

Apply $\hat{H}_{\mathrm{cpl}}$ to $|\psi\rangle$:

$$\hat{H}_{\mathrm{cpl}} |\psi\rangle = \frac{\hbar}{2} \left(\Omega_1 |3\rangle\langle 1| + \Omega_2 |3\rangle\langle 2|\right)\left(a\,|1\rangle + b\,|2\rangle\right) + \frac{\hbar}{2} \left(\Omega_1^* |1\rangle\langle 3| + \Omega_2^* |2\rangle\langle 3|\right)|\psi\rangle\,. \tag{17}$$

But $\langle 3|\psi\rangle = 0$ since $|\psi\rangle$ has no $|3\rangle$ component, so the h.c. part vanishes on $|\psi\rangle$. Thus

$$\hat{H}_{\text{cpl}}|\psi\rangle = \frac{\hbar}{2}\left(\Omega_1 a|3\rangle + \Omega_2 b|3\rangle\right) = \frac{\hbar}{2}\left(\Omega_1 a + \Omega_2 b\right)|3\rangle\,. \tag{18}$$

Therefore, the condition for *no coupling to* $|3\rangle$ is

$$\Omega_1 a + \Omega_2 b = 0. \tag{19}$$

Solve for (a, b):

$$b = -\frac{\Omega_1}{\Omega_2}a.$$

Choose $a = \Omega_2$ and $b = -\Omega_1$ (overall scale is irrelevant), giving the unnormalized dark state:

$$|D\rangle \propto \Omega_2|1\rangle - \Omega_1|2\rangle\,.$$

Normalize:

$$\boxed{|D\rangle = \frac{\Omega_2|1\rangle - \Omega_1|2\rangle}{\sqrt{|\Omega_1|^2 + |\Omega_2|^2}}.} \tag{20}$$

Key point: Meaning of the dark state

The system is trapped in a coherent superposition of $|1\rangle$ and $|2\rangle$ such that excitation amplitudes cancel. This is the essence of CPT/EIT in a Λ system.

3.3 Two-photon resonance condition for a *stationary* dark state

Even if $|D\rangle$ is uncoupled from $|3\rangle$, the lower states can accumulate relative phase if their effective energies differ in the rotating frame. From (14), the term $-\hbar\delta\,|2\rangle\langle 2|$ causes relative phase evolution between $|1\rangle$ and $|2\rangle$ unless $\delta = 0$.

Thus the perfect stationary CPT condition is:

$$\boxed{\delta = 0 \quad \text{(two-photon resonance).}} \tag{21}$$

Logic note (for lecture): What to say out loud

"One-photon detuning affects how strongly we excite the bright states, but two-photon detuning determines whether the dark superposition remains dark over time."

Common pitfall: Coherent vs incoherent "dark"

In CPT, darkness is *coherent interference*. In many solid defects (including NV), darkness often arises from *shelving into metastable singlets* (incoherent). Do not mix these mechanisms.

4 Defect centers as multi-level emitters: why "TLS" is rarely enough

4.1 Why solid-state color centers are not ideal TLS

A solid-state defect has:

- electronic ground/excited manifolds (often with spin sublevels),
- phonon sidebands (vibronic coupling),
- intersystem crossing (ISC) into metastable states,
- charge conversion between different charge states (e.g., NV^- and NV^0).

Logic note (for lecture): Core message

Even when we *use* a "two-level transition" for optics, extra states control brightness, spin polarization, and readout contrast. These extra states are the origin of dark states in practice.

5 NV centers in diamond: charge states and level structure

5.1 NV charge states (full picture at the level needed for ODMR)

The nitrogen-vacancy defect can exist in different charge states, most notably:

- NV^- (negative): most used for spin qubit + ODMR magnetometry.
- NV^0 (neutral): different optical transitions and typically lower ODMR usefulness.
- NV^+ (positive): can exist under certain doping/illumination conditions (less common in standard ODMR experiments).

Info: Charge conversion (conceptual)

Optical illumination can ionize or recombine the defect:

$$NV^- \rightleftharpoons NV^0,$$

which changes fluorescence spectrum and can reduce effective ODMR contrast if not controlled. We will focus on NV^- for the spin/ODMR model.

5.2 NV^- electronic structure: triplet–triplet + singlet shelf

NV^- has:

- Ground triplet: ${}^3A_2$ with spin $S = 1$ and sublevels $m_s = 0, \pm 1$.
- Excited triplet: ${}^3E$ with $S = 1$ and sublevels $m_s = 0, \pm 1$.
- Intermediate singlet manifold: often drawn as ${}^1A_1$ and ${}^1E$ (metastable), responsible for spin-dependent ISC and optical pumping.

Logic note (for lecture): Why singlets matter

The singlet shelf is the *incoherent dark pathway*: it reduces fluorescence and, crucially, does so more strongly for $m_s = \pm 1$ than for $m_s = 0$. This creates ODMR contrast.

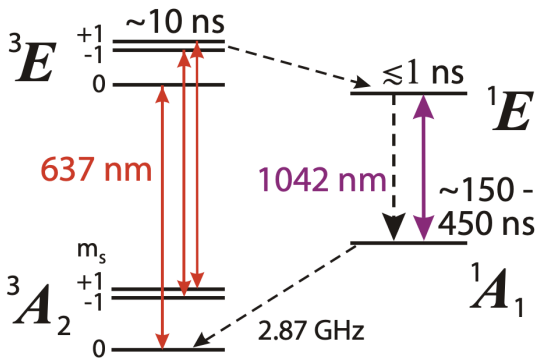

Figure 2: Level diagram for NV center showing spin-triplet ground and excited states, as well as the singlet system involved in intersystem crossing. Radiative transitions are indicated by solid arrows and non-radiative transitions by dashed arrows.

5.3 Ground-state spin Hamiltonian: zero-field splitting + Zeeman

In the NV^- ground triplet, the effective spin Hamiltonian is commonly written as

$$\boxed{\hat{H}_{\text{spin}} = \hbar D \hat{S}_z^2 + \hbar E(\hat{S}_x^2 - \hat{S}_y^2) + \hbar \gamma_e \boldsymbol{B} \cdot \hat{\boldsymbol{S}}.} \tag{22}$$

Here:

- D is the zero-field splitting parameter (splits $m_s = 0$ from $m_s = \pm 1$ even at $B = 0$),
- E encodes strain/electric-field splitting of the ± 1 manifold,
- γ_e is the electron gyromagnetic ratio,
- $\hat{\boldsymbol{S}}$ are spin-1 operators.

Simplified case: $E \approx 0$ and $\boldsymbol{B} \parallel \hat{z}$ (NV axis). Then $\boldsymbol{B} \cdot \hat{\boldsymbol{S}} = B_z \hat{S}_z$. Since $\hat{S}_z |m_s\rangle = m_s |m_s\rangle$ and $\hat{S}_z^2 |m_s\rangle = m_s^2 |m_s\rangle$, the energies are

$$E(m_s = 0)/\hbar = D \cdot 0^2 + \gamma_e B_z \cdot 0 = 0, \tag{23}$$

$$E(m_s = +1)/\hbar = D \cdot 1^2 + \gamma_e B_z \cdot (+1) = D + \gamma_e B_z, \tag{24}$$

$$E(m_s = -1)/\hbar = D \cdot 1^2 + \gamma_e B_z \cdot (-1) = D - \gamma_e B_z. \tag{25}$$

Therefore the transition angular frequencies from $m_s = 0$ are

$$\boxed{\omega_\pm = D \pm \gamma_e B_z \quad (E \approx 0,\ \boldsymbol{B} \parallel \text{NV}).} \tag{26}$$

Key point: Magnetometry principle

Measure $\omega_\pm$ (via ODMR). Then B_z follows from frequency splitting:

$$B_z = \frac{\omega_+ - \omega_-}{2\gamma_e}.$$

6 Selection rules and the origin of spin-dependent fluorescence

6.1 Optical selection (qualitative rule used in ODMR modeling)

To a good approximation:

- Optical transitions are mostly spin-conserving: $\Delta m_s \approx 0$ for ${}^3A_2 \leftrightarrow {}^3E$.
- ISC to singlets is spin-dependent: excited $m_s = \pm 1$ has higher probability to undergo ISC than excited $m_s = 0$.
- Singlet decay preferentially repopulates ground $m_s = 0$ (optical pumping / spin polarization).

Logic note (for lecture): Practical effect

Under continuous green excitation, population accumulates in ground $m_s = 0$ (bright). If microwaves drive $m_s = 0 \leftrightarrow m_s = \pm 1$, some population is transferred into the "dim" branch and fluorescence drops: that is ODMR.

7 Effective multi-level rate-equation model for NV^- fluorescence

7.1 Choose a minimal 5-level model

We compress $m_s = \pm 1$ into a single "spin-1" manifold label to keep math manageable:

Info: Effective 5-level basis

Ground triplet:

$$g_0 \equiv \left|{}^3A_2, m_s = 0\right\rangle, \qquad g_1 \equiv \left|{}^3A_2, m_s = \pm 1\right\rangle \text{ (lumped).}$$

Excited triplet:

$$e_0 \equiv \left|{}^3E, m_s = 0\right\rangle, \qquad e_1 \equiv \left|{}^3E, m_s = \pm 1\right\rangle \text{ (lumped).}$$

Metastable singlet shelf:

$$s \equiv \text{effective singlet state (lumped).}$$

Let populations be

$$p_{g0}, p_{g1}, p_{e0}, p_{e1}, p_s, \qquad p_{g0} + p_{g1} + p_{e0} + p_{e1} + p_s = 1.$$

7.2 Define rates

We define:

- Optical excitation (green pump) from ground to excited:

$$g_0 \xrightarrow{k_{\text{exc}}} e_0, \qquad g_1 \xrightarrow{k_{\text{exc}}} e_1.$$

- Radiative decay (fluorescence) from excited to ground (spin-conserving dominant):

$$e_0 \xrightarrow{k_r} g_0, \qquad e_1 \xrightarrow{k_r} g_1.$$

- Intersystem crossing (ISC) from excited to singlet (spin-dependent):

$$e_0 \xrightarrow{k_{isc}^{(0)}} s, \qquad e_1 \xrightarrow{k_{isc}^{(1)}} s,$$

  with typically $k_{isc}^{(1)} \gg k_{isc}^{(0)}$.

- Singlet decay back to ground (spin-polarizing):

$$s \xrightarrow{k_{s0}} g_0, \qquad s \xrightarrow{k_{s1}} g_1,$$

  typically $k_{s0} > k_{s1}$ (bias toward g_0).

Logic note (for lecture): Why lumping still works

For ODMR contrast, we only need a "bright" ground state ($m_s = 0$) and a "dim" manifold ($m_s = \pm 1$). The key asymmetry is in ISC rates.

7.3 Write rate equations explicitly (matrix-ready)

The population dynamics:

$$\dot{p}_{g0} = -k_{\text{exc}} p_{g0} + k_r p_{e0} + k_{s0} p_s + \underbrace{R_{\text{mw}}(p_{g1} - p_{g0})}_{\text{MW mixing}}, \tag{27}$$

$$\dot{p}_{g1} = -k_{\text{exc}} p_{g1} + k_r p_{e1} + k_{s1} p_s + \underbrace{R_{\text{mw}}(p_{g0} - p_{g1})}_{\text{MW mixing}}, \tag{28}$$

$$\dot{p}_{e0} = +k_{\text{exc}} p_{g0} - (k_r + k_{isc}^{(0)}) p_{e0}, \tag{29}$$

$$\dot{p}_{e1} = +k_{\text{exc}} p_{g1} - (k_r + k_{isc}^{(1)}) p_{e1}, \tag{30}$$

$$\dot{p}_s = +k_{isc}^{(0)} p_{e0} + k_{isc}^{(1)} p_{e1} - (k_{s0} + k_{s1}) p_s. \tag{31}$$

Info: Microwave mixing as an effective rate

A fully coherent MW drive is described by Bloch equations. In a simplified fluorescence-rate model, its net effect is to equalize g_0 and g_1 at a rate

$$R_{\text{mw}}(\omega) \sim \frac{\Omega_{\text{mw}}^2}{\Gamma_2} \cdot \frac{(\Gamma_2/2)^2}{(\omega - \omega_0)^2 + (\Gamma_2/2)^2},$$

where Ω_{mw} is MW Rabi frequency, $\Gamma_2 = 1/T_2^*$ (effective dephasing), and ω_0 is the spin transition frequency. We will use this to get ODMR lineshapes.

7.4 Steady-state solution: eliminate excited and singlet populations algebraically

For continuous-wave (CW) ODMR, we care about steady state:

$$\dot{p}_{g0} = \dot{p}_{g1} = \dot{p}_{e0} = \dot{p}_{e1} = \dot{p}_s = 0.$$

7.4.1 Step 1: solve for p_{e0}, p_{e1} from (29)–(30)

Set (29)=0:

$$0 = k_{\rm exc} p_{g0} - (k_r + k_{isc}^{(0)}) p_{e0} \quad \Rightarrow \quad \boxed{p_{e0} = \frac{k_{\rm exc}}{k_r + k_{isc}^{(0)}}\, p_{g0}.} \tag{32}$$

Similarly:

$$\boxed{p_{e1} = \frac{k_{\rm exc}}{k_r + k_{isc}^{(1)}}\, p_{g1}.} \tag{33}$$

7.4.2 Step 2: solve for p_s from (31)

Set (31)=0 and substitute (32)–(33):

$$0 = k_{isc}^{(0)} p_{e0} + k_{isc}^{(1)} p_{e1} - (k_{s0} + k_{s1}) p_s \tag{34}$$

$$\Rightarrow \quad p_s = \frac{k_{isc}^{(0)} p_{e0} + k_{isc}^{(1)} p_{e1}}{k_{s0} + k_{s1}}$$

$$= \frac{1}{k_{s0} + k_{s1}} \left[k_{isc}^{(0)} \frac{k_{\rm exc}}{k_r + k_{isc}^{(0)}} p_{g0} + k_{isc}^{(1)} \frac{k_{\rm exc}}{k_r + k_{isc}^{(1)}} p_{g1} \right]. \tag{35}$$

7.4.3 Step 3: reduce to two variables (p_{g0}, p_{g1})

Define for compactness

$$a_0 \equiv \frac{k_{\rm exc}}{k_r + k_{\rm isc}^{(0)}}, \qquad a_1 \equiv \frac{k_{\rm exc}}{k_r + k_{\rm isc}^{(1)}}.$$

Then (32)–(33) become

$$p_{e0} = a_0\, p_{g0}, \qquad p_{e1} = a_1\, p_{g1}.$$

Also define

$$b_0 \equiv \frac{k_{\rm isc}^{(0)}\, k_{\rm exc}}{(k_r + k_{\rm isc}^{(0)})(k_{s0} + k_{s1})}, \qquad b_1 \equiv \frac{k_{\rm isc}^{(1)}\, k_{\rm exc}}{(k_r + k_{\rm isc}^{(1)})(k_{s0} + k_{s1})},$$

so that (35) reads

$$p_s = b_0\, p_{g0} + b_1\, p_{g1}.$$

Now substitute these into the steady-state ground-state equation (27):

$$0 = -k_{\rm exc} p_{g0} + k_r p_{e0} + k_{s0} p_s + R_{\rm mw}(p_{g1} - p_{g0}).$$

Using $p_{e0} = a_0 p_{g0}$ and $p_s = b_0 p_{g0} + b_1 p_{g1}$ gives

$$0 = [-k_{\rm exc} + k_r a_0 + k_{s0} b_0 - R_{\rm mw}]\, p_{g0} + [k_{s0} b_1 + R_{\rm mw}]\, p_{g1}.$$

It is useful to simplify the coefficients by defining

$$\alpha_0 \equiv \frac{k_{\rm exc}\, k_{\rm isc}^{(0)}\, k_{s1}}{(k_r + k_{\rm isc}^{(0)})(k_{s0} + k_{s1})}, \qquad \alpha_1 \equiv \frac{k_{\rm exc}\, k_{\rm isc}^{(1)}\, k_{s0}}{(k_r + k_{\rm isc}^{(1)})(k_{s0} + k_{s1})}.$$

Then the ground-state balance becomes

$$(\alpha_0 + R_{\mathrm{mw}})\, p_{g0} = (\alpha_1 + R_{\mathrm{mw}})\, p_{g1}. \tag{35a}$$

Hence

$$\frac{p_{g1}}{p_{g0}} = \frac{\alpha_0 + R_{\mathrm{mw}}}{\alpha_1 + R_{\mathrm{mw}}}. \tag{35b}$$

Now use normalization:

$$p_{g0} + p_{g1} + p_{e0} + p_{e1} + p_s = 1.$$

Substituting the eliminated populations gives

$$(1 + a_0 + b_0)p_{g0} + (1 + a_1 + b_1)p_{g1} = 1.$$

Define

$$A_0 \equiv 1 + a_0 + b_0, \qquad A_1 \equiv 1 + a_1 + b_1.$$

Then

$$A_0 p_{g0} + A_1 p_{g1} = 1. \tag{35c}$$

Solving (35a) and (35c) yields the steady-state ground populations:

$$p_{g0} = \frac{\alpha_1 + R_{\mathrm{mw}}}{A_0(\alpha_1 + R_{\mathrm{mw}}) + A_1(\alpha_0 + R_{\mathrm{mw}})}, \tag{35d}$$

$$p_{g1} = \frac{\alpha_0 + R_{\mathrm{mw}}}{A_0(\alpha_1 + R_{\mathrm{mw}}) + A_1(\alpha_0 + R_{\mathrm{mw}})}. \tag{35e}$$

The eliminated excited and singlet populations then follow immediately from

$$p_{e0} = a_0 p_{g0}, \qquad p_{e1} = a_1 p_{g1}, \qquad p_s = b_0 p_{g0} + b_1 p_{g1}.$$

Key point: Interpretation of the solution

Without microwaves ($R_{\mathrm{mw}} = 0$), the ratio $p_{g1}/p_{g0} = \alpha_0/\alpha_1$ is set by optical pumping and spin-dependent shelving, and typically favors $g0$. As R_{mw} increases, the microwave drive tends to equalize the two ground manifolds, pushing more population into the dim branch and reducing fluorescence.

7.5 Fluorescence signal expression

Detected fluorescence rate is proportional to radiative decays:

$$F \propto k_r(p_{e0} + p_{e1}). \tag{36}$$

Using $p_{e0} = a_0 p_{g0}$ and $p_{e1} = a_1 p_{g1}$ gives

$$F \propto k_r \left(a_0 p_{g0} + a_1 p_{g1}\right). \tag{37}$$

Substituting the explicit steady-state populations (35d)–(35e),

$$F \propto k_r \frac{a_0(\alpha_1 + R_{\mathrm{mw}}) + a_1(\alpha_0 + R_{\mathrm{mw}})}{A_0(\alpha_1 + R_{\mathrm{mw}}) + A_1(\alpha_0 + R_{\mathrm{mw}})}.$$

Equivalently, define

$$N_0 \equiv a_0\alpha_1 + a_1\alpha_0, \qquad N_1 \equiv a_0 + a_1,$$

$$D_0 \equiv A_0\alpha_1 + A_1\alpha_0, \qquad D_1 \equiv A_0 + A_1.$$

Then the fluorescence takes the compact form

$$F(R_{\mathrm{mw}}) \propto k_r \, \frac{N_0 + N_1 R_{\mathrm{mw}}}{D_0 + D_1 R_{\mathrm{mw}}}. \tag{37a}$$

Useful limits

- **Off resonance / no MW** ($R_{\mathrm{mw}} = 0$):

$$F_{\mathrm{off}} \propto k_r \, \frac{N_0}{D_0}.$$

- **Strong resonant MW** ($R_{\mathrm{mw}} \gg \alpha_0, \alpha_1$):

$$F_{\mathrm{on}} \propto k_r \, \frac{N_1}{D_1}.$$

Because typically

$$k_{\mathrm{isc}}^{(1)} \gg k_{\mathrm{isc}}^{(0)},$$

the $g1 \to e1 \to s$ pathway is more strongly shelved and therefore emits less fluorescence. As a result,

$$F_{\mathrm{on}} < F_{\mathrm{off}},$$

which is the origin of the ODMR dip.

Connection to ODMR lineshape

From the box above, the microwave mixing rate is frequency dependent:

$$R_{\mathrm{mw}}(\omega) \sim \frac{\Omega_{\mathrm{mw}}^2}{\Gamma_2} \frac{(\Gamma_2/2)^2}{(\omega - \omega_0)^2 + (\Gamma_2/2)^2}.$$

Therefore $F(\omega) = F(R_{\mathrm{mw}}(\omega))$ inherits a dip centered at ω_0. For weak-to-moderate microwave drive, one may expand (37a) around $R_{\mathrm{mw}} = 0$, which leads to the familiar Lorentzian ODMR form used in the next section:

$$F(\omega) \approx F_0 \left[1 - C \, \frac{(\Gamma/2)^2}{(\omega - \omega_0)^2 + (\Gamma/2)^2}\right].$$

Key point: Why fluorescence depends on spin

The practical steady-state equation (37a) makes the physics explicit: microwaves increase the population of the $m_s = \pm 1$ manifold, that manifold shelves more strongly into the singlet, and the total radiative fluorescence therefore decreases.

8 ODMR: microwave resonance seen as a fluorescence dip

8.1 Microwave-driven ground-state transition (coherent picture)

Inside the ground manifold, we can treat $\{g_0, g_1\}$ as an effective TLS (spin qubit):

$$|0\rangle \equiv g_0, \qquad |1\rangle \equiv g_1.$$

A microwave drive near ω_0 produces (RWA) Hamiltonian

$$\hat{H}_{\rm mw}^{\rm (rot)} = \frac{\hbar}{2}\left(\Delta_{\rm mw}\sigma_z + \Omega_{\rm mw}\sigma_x\right), \qquad \Delta_{\rm mw} = \omega_{\rm mw} - \omega_0. \tag{36}$$

In the presence of dephasing T_2^* and relaxation T_1, Bloch equations predict a Lorentzian steady-state response. For fluorescence modeling, we capture this by an effective mixing rate $R_{\rm mw}(\omega)$ (previous box).

8.2 ODMR lineshape (semi-analytic)

Near the resonance, the MW-induced transfer $g_0 \leftrightarrow g_1$ is strongest. This increases shelving and decreases fluorescence, giving a dip:

$$\boxed{F(\omega_{\rm mw}) = F_0\left[1 - C\frac{(\Gamma/2)^2}{(\omega_{\rm mw}-\omega_0)^2 + (\Gamma/2)^2}\right].} \tag{37}$$

Here:

- F_0 is off-resonant fluorescence (MW far detuned),
- C is ODMR contrast (fractional dip depth),
- Γ is the linewidth (set by T_2^* and power broadening).

Logic note (for lecture): Connect rate model to dip formula

$R_{\rm mw}(\omega)$ is Lorentzian in ω; $R_{\rm mw}$ controls how much population moves into the dim channel; therefore fluorescence inherits a Lorentzian dip.

8.3 Power broadening (useful scaling)

In many driven TLS systems, the effective linewidth grows with drive:

$$\boxed{\Gamma \approx \Gamma_0\sqrt{1 + \left(\frac{\Omega_{\rm mw}}{\Gamma_0}\right)^2},} \tag{38}$$

where Γ_0 is the intrinsic linewidth (set by dephasing and relaxation) in the weak-drive limit.

Common pitfall: Practical trade-off

Increasing MW power increases signal slope (good) but also broadens the line (bad). Optimal sensitivity occurs at an intermediate power.

9 Magnetic-field measurement with ODMR

9.1 Zeeman shift to field conversion

From (26), when B is aligned with the NV axis:

$$\omega_\pm = D \pm \gamma_e B_z.$$

Hence:

$$B_z = \frac{\omega_+ - \omega_-}{2\gamma_e}. \tag{41}$$

If only one branch is measured (e.g., choose the $m_s = 0 \to +1$ transition),

$$B_z = \frac{\omega_+ - D}{\gamma_e}. \tag{42}$$

9.2 Small-signal magnetometry: slope method

To make the signal definition precise, let

$$R(\omega)$$

denote the detected fluorescence *count rate* (photons/s), and let

$$N(\omega;\tau) = R(\omega)\tau$$

denote the total number of detected photons collected in an integration time τ.

Since the transition frequency depends on magnetic field, small changes obey

$$\delta\omega = \gamma_e\,\delta B.$$

Therefore the corresponding change in the measured photon number is

$$\delta N \approx \frac{\partial N}{\partial \omega}\,\delta\omega = \frac{\partial N}{\partial \omega}\,\gamma_e\,\delta B.$$

Solving for δB gives

$$\delta B \approx \frac{\delta N}{\left|\frac{\partial N}{\partial \omega}\right|\gamma_e}. \tag{43}$$

Because $N = R\tau$, we also have

$$\frac{\partial N}{\partial \omega} = \tau\frac{\partial R}{\partial \omega}.$$

Thus one may equivalently write

$$\delta B \approx \frac{\delta N}{\tau\left|\frac{\partial R}{\partial \omega}\right|\gamma_e}. \tag{44}$$

9.3 Shot-noise limited sensitivity (standard scaling)

If photon shot noise dominates, then the photon-number uncertainty in time τ is

$$\delta N \sim \sqrt{N} = \sqrt{R\tau}.$$

Define magnetic sensitivity as the noise-equivalent magnetic field referred to a 1 Hz measurement bandwidth:

$$\eta_B \equiv \delta B\sqrt{\tau}.$$

Using (44),

$$\eta_B = \frac{\delta N}{\tau\left|\frac{\partial R}{\partial \omega}\right|\gamma_e}\sqrt{\tau}.$$

Substitute $\delta N \sim \sqrt{R\tau}$:

$$\eta_B \sim \frac{\sqrt{R\tau}}{\tau \left|\frac{\partial R}{\partial \omega}\right| \gamma_e} \sqrt{\tau} = \frac{\sqrt{R}}{\left|\frac{\partial R}{\partial \omega}\right| \gamma_e}. \tag{45}$$

Now use the Lorentzian ODMR dip written in (39), but expressed as a count rate:

$$R(\omega_{\mathrm{mw}}) = R_0 \left[1 - C \frac{(\Gamma/2)^2}{(\omega_{\mathrm{mw}} - \omega_0)^2 + (\Gamma/2)^2}\right].$$

Its slope is

$$\frac{\partial R}{\partial \omega_{\mathrm{mw}}} = R_0 C \, \frac{2(\omega_{\mathrm{mw}} - \omega_0)(\Gamma/2)^2}{[(\omega_{\mathrm{mw}} - \omega_0)^2 + (\Gamma/2)^2]^2}.$$

The maximum slope magnitude occurs at

$$|\omega_{\mathrm{mw}} - \omega_0| = \frac{\Gamma}{2\sqrt{3}},$$

for which the exact numerical prefactor is unimportant for scaling. Therefore,

$$\left|\frac{\partial R}{\partial \omega}\right|_{\max} \sim \frac{R_0 C}{\Gamma}.$$

Substituting this into (45) gives the standard shot-noise-limited scaling

$$\eta_B \sim \frac{\Gamma}{C \, \gamma_e \sqrt{R_0}}. \tag{46}$$

Key point: Sensitivity intuition

Better magnetometry requires:

narrower linewidth ($\Gamma \downarrow$), higher contrast ($C \uparrow$), more photons ($R \uparrow$).

10 Connecting back to dark states: NV shelving vs coherent CPT

10.1 Incoherent dark state in NV: shelving mechanism

In the NV model, the singlet s is a metastable level that reduces fluorescence:

$$e_1 \xrightarrow{k_{isc}^{(1)}} s \xrightarrow{k_{s0}, k_{s1}} g_{0/1}.$$

During time spent in s, no radiative photons are emitted in the main fluorescence band.

Info: Why call it "dark"?

Because population in s is temporarily invisible to fluorescence detection: it is *dark* to the optical cycling transition.

10.2 Coherent dark state in a Λ system: CPT

In contrast, CPT dark state (20) is a coherent superposition:

$$|D\rangle = \frac{\Omega_2 |1\rangle - \Omega_1 |2\rangle}{\sqrt{|\Omega_1|^2 + |\Omega_2|^2}},$$

which is dark because *excitation amplitudes interfere destructively.*

Common pitfall: Do not confuse the mechanisms

Shelving darkness: depends on incoherent rates and metastable lifetimes.
CPT darkness: depends on phase coherence and two-photon resonance $\delta = 0$.

11 Bloch-sphere wrap-up: ODMR as Bloch dynamics + optical pumping

11.1 Ground-state qubit Bloch sphere

Treat $\{g_0, g_1\}$ as a qubit:

$$|\psi\rangle = c_0 |0\rangle + c_1 |1\rangle, \qquad |c_0|^2 + |c_1|^2 = 1.$$

Parameterize:

$$c_0 = \cos\frac{\theta}{2}, \qquad c_1 = e^{i\phi} \sin\frac{\theta}{2}. \tag{39}$$

Bloch vector $\boldsymbol{s} = (\langle\sigma_x\rangle, \langle\sigma_y\rangle, \langle\sigma_z\rangle)$:

$$s_x = \sin\theta\cos\phi, \qquad s_y = \sin\theta\sin\phi, \qquad s_z = \cos\theta. \tag{40}$$

11.2 Microwave as coherent rotation; optical pumping as non-unitary flow

From (36), MW drive causes rotations around an effective axis:

$$\boldsymbol{\Omega}_{\text{eff}} = (\Omega_{\text{mw}},\, 0,\, \Delta_{\text{mw}}).$$

Optical pumping + ISC acts like relaxation that pushes the Bloch vector toward $|0\rangle$ (spin polarization).

Logic note (for lecture): Final big-picture sentence

ODMR is a hybrid process: **coherent MW rotations** compete with **incoherent optical pumping and shelving**. The measured signal is fluorescence, which encodes the steady-state spin polarization.

One-page recall sheet (last slide)

- **TLS:** driven Hamiltonian $\hat{H}^{(\text{rot})} = \frac{\hbar}{2}(\Delta\sigma_z + \Omega\sigma_x)$.
- **3LS:** Λ systems support **coherent dark state** $|D\rangle = (\Omega_2 |1\rangle - \Omega_1 |2\rangle)/\sqrt{|\Omega_1|^2 + |\Omega_2|^2}$, stationary when $\delta = 0$.

- **NV^- levels:** ${}^3A_2$ ground ($m_s = 0, \pm 1$), ${}^3E$ excited, singlet shelf produces spin-dependent fluorescence.
- **Spin Hamiltonian:** $\hat{H} = \hbar D S_z^2 + \hbar \gamma_e \boldsymbol{B} \cdot \boldsymbol{S}$ (plus strain term).
- **Zeeman shift:** $\omega_\pm = D \pm \gamma_e B_z$ for B along NV axis.
- **ODMR:** MW resonance increases population in dim channel $\Rightarrow$ fluorescence dip $F(\omega) = F_0 \left[1 - C \frac{(\Gamma/2)^2}{(\omega-\omega_0)^2+(\Gamma/2)^2}\right]$.
- **Sensitivity scaling:** $\eta_B \sim \Gamma/(C\gamma_e\sqrt{R})$.
- **Bloch sphere:** MW drives rotations; optical pumping drives polarization to $|0\rangle$.

12 Applications of Three-Level Systems in Quantum Technologies

12.1 Motivation: why three-level systems matter in quantum technology

Three-level systems appear naturally in many quantum platforms including alkali atoms, trapped ions, neutral atoms, rare-earth crystals, and solid-state defect centers. The presence of an additional level enables new phenomena beyond the simple two-level atom discussed earlier.

Key capabilities enabled by three-level systems include

- coherent population trapping (CPT),
- electromagnetically induced transparency (EIT),
- Raman transitions between long-lived ground states,
- optical pumping and spin polarization,
- strong light–matter nonlinearities.

These effects form the basis of several quantum technologies such as

- quantum memories,
- atomic clocks,
- quantum magnetometers,
- quantum computing platforms.

Key conceptual point

The importance of three-level systems is not merely the presence of an additional energy level. Rather, the additional level enables **interference between multiple excitation pathways** and **population transfer between long-lived states**.

12.2 Λ systems: Raman transitions for qubit control

One important application of Λ systems is coherent population transfer between two ground states via a Raman process.

Consider again the Λ configuration with states

$$|1\rangle, \quad |2\rangle \quad \text{(ground states)}$$

$$|3\rangle \quad \text{(excited state)}.$$

Two classical optical fields drive the transitions

$$|1\rangle \leftrightarrow |3\rangle, \qquad |2\rangle \leftrightarrow |3\rangle.$$

Let the corresponding Rabi frequencies be

$$\Omega_1, \qquad \Omega_2.$$

Assume both lasers are detuned from the excited state by a large detuning Δ:

$$\Delta \gg |\Omega_1|, |\Omega_2|.$$

In this regime the excited state is only *virtually populated*. The dynamics can therefore be reduced to an effective two-level system between $|1\rangle$ and $|2\rangle$.

Adiabatic elimination of the excited state yields the effective Hamiltonian

$$\hat{H}_{\text{eff}} = \frac{\hbar}{2} \left(\Omega_{\text{eff}} |1\rangle\langle 2| + \Omega_{\text{eff}}^* |2\rangle\langle 1| \right),$$

where the effective Raman Rabi frequency is

$$\Omega_{\text{eff}} = \frac{\Omega_1 \Omega_2^*}{2\Delta}.$$

Logic note

Even though the excited state $|3\rangle$ mediates the interaction, it remains essentially unpopulated when the detuning is large. This suppresses spontaneous emission and enables high-fidelity coherent control of the ground-state qubit.

Quantum technology applications Raman Λ transitions are widely used in

- trapped-ion quantum computers,
- neutral-atom optical tweezer arrays,
- spin control in solid-state defects such as NV centers.

12.3 Λ systems: atomic clocks via coherent population trapping

Another major application of Λ systems is the realization of extremely stable frequency references using coherent population trapping.

Consider two optical fields driving transitions from the two ground states to the same excited state.

Let the laser frequencies be

$$\omega_1, \qquad \omega_2.$$

Define the hyperfine splitting between the ground states

$$\omega_{12} = \frac{E_2 - E_1}{\hbar}.$$

A dark-state resonance occurs when

$$\omega_1 - \omega_2 = \omega_{12}.$$

At this condition the system enters the coherent superposition

$$|D\rangle = \frac{\Omega_2|1\rangle - \Omega_1|2\rangle}{\sqrt{|\Omega_1|^2 + |\Omega_2|^2}},$$

which was derived earlier for the Λ system.

Because the excited state is not populated, absorption vanishes and a sharp resonance appears in the transmission spectrum.

Info: CPT clocks

Chip-scale atomic clocks (CSAC) operate by locking the frequency difference between two lasers or microwave sidebands to the CPT resonance of alkali atoms such as rubidium or cesium.

12.4 Λ systems: atomic magnetometry

In atomic magnetometers the Λ configuration is used to measure magnetic-field-induced splitting of the ground states.

A magnetic field B causes a Zeeman shift

$$\omega_{12} = g\mu_B B,$$

where g is the Landé g-factor and μ_B is the Bohr magneton.

The CPT resonance condition becomes

$$\omega_1 - \omega_2 = g\mu_B B.$$

Thus the magnetic field can be obtained directly from the measured frequency difference:

$$B = \frac{\omega_1 - \omega_2}{g\mu_B}.$$

Key point

The Λ system converts a magnetic-field-induced energy shift into a measurable optical resonance frequency.

Atomic magnetometers based on this principle can reach sensitivities in the femtotesla range.

12.5 V systems: Autler–Townes spectroscopy

In a V-type configuration a single ground state is coupled to two excited states:

$$|1\rangle \leftrightarrow |2\rangle, \qquad |1\rangle \leftrightarrow |3\rangle.$$

A strong laser driving the transition $|1\rangle \leftrightarrow |2\rangle$ with Rabi frequency Ω modifies the energy spectrum of the atom.

The dressed-state picture predicts a splitting of the excited state into two levels separated approximately by

$$\Delta E \approx \hbar\Omega.$$

When a probe laser scans the second transition $|1\rangle \leftrightarrow |3\rangle$, two absorption peaks appear.

This phenomenon is known as the **Autler–Townes splitting**.

Experimental use

Autler–Townes spectroscopy is commonly used to measure transition dipole moments and Rabi frequencies in atomic and solid-state systems.

12.6 Cascade (Ξ) systems: Rydberg quantum gates

Cascade systems have a ladder structure

$$|1\rangle \leftrightarrow |2\rangle \leftrightarrow |3\rangle.$$

In neutral-atom experiments the levels are typically

$$|1\rangle = 5S_{1/2}, \qquad |2\rangle = 5P_{3/2}, \qquad |3\rangle = nS \text{ (Rydberg state)}.$$

Rydberg states possess extremely large electric dipole moments. As a result, two atoms simultaneously excited to Rydberg states experience strong dipole–dipole interactions.

This leads to the **Rydberg blockade** effect: excitation of one atom prevents nearby atoms from being excited.

Quantum computing application

The Rydberg blockade mechanism enables fast entangling gates between neutral atoms and forms the basis of several scalable neutral-atom quantum computing architectures.

12.7 Summary of applications

System type	Physical mechanism	Quantum technology
Λ	CPT / EIT	Quantum memories
Λ	Raman transitions	Qubit control
Λ	CPT resonance	Atomic clocks
Λ	Zeeman splitting	Magnetometers
V	Autler–Townes splitting	Spectroscopy
Ξ	Rydberg excitation	Neutral-atom quantum computing

Final takeaway

Three-level systems are fundamental building blocks in quantum technology because they enable coherent control, interference, and long-lived quantum-state storage that cannot be realized with simple two-level atoms.